ACTIVE CONTROL EXPERIMENTAL INVESTIGATION ABOUT AERODYNAMIC CHARACTERISTICS AT HIGH INCIDENCE

Yang Yongnian* Yu Xinzhi* Wang Zongdong+ Li Jiangying**

Aerodynamic Research Institute
Northwestern Polytechnical University
Xi'an, 710072,
CHINA

Abstract

In this paper, three experimental schemes of active control for asymmetric force, controlable rotating nose-tip, controlable blowing jet at nose and controlable strake, in a low speed wind tunnel are discussed. The investigated models are 60mm diameter cylinder with a tangent ogive nose, 60mm diameter cylinder with a cone and an aircraft model with strakes respectively.The active control devices are designed.The control laws are investigated.

The experimental results show that the asymmetric forces at high angle of attack are reduced significantly for all experimental schemes. The developed active control programs can automatically limit the side force on the models to its minimum magnitude. The schemes of controlable blowing jet and controlable strake can be adopted to enhanced the lateral maneuverability.

Nomenclature

C_L Lift coefficient=Lift/qs
C_y Side force coefficient= Side force/qs
C_n Yawing moment coefficient= Yawing moment/qsb
C_l Rolling moment coefficient= Rolling moment/qsb
C_x Resistance coefficient= Resistance/qs
α Angle of attack (deg)
δ Deflection of strake (deg)
n Rotating rate of the nose-tip(Hz)
C_j Blowing jet coefficient
S Reference area (cross section area of cylinder or wing area)
q Freestream dynamic pressure
b Reference length (diameter of cylinder or average aerodynamic chord of wing)

Subscript
L Left
R Right

Introduction

In high incidence flight, symmetrical aircraft and missile may be subjected to asymmetric forces because of vortex wake asymmetry .The asymmetric vortex on the wake can bring about serious control problem for aircraft and missile flying at high incidence due to their large magnitudes coupled with sudden change in direction. In this field, the aerodynamicist have done a great deal of research work[1--8]. To alleviate the asymmetric forces various methods, such as roughness strips,fixed strakes and change nose shape etc., are presented . These methods raise the onset angle and alleviate the asymmetric forces but their efficiency is only at the certain range of incidence.

It is well know that the active control technology have been used in high performance aircraft in many aspects. Various active control system, such as active control augmentation system, direct forces control, gust alleviation and flutter suppression, are widely investigated. The active control technology is a good way to control the asymmetric force at high incidence. Some concept of active control for asymmetric force , such as hinged strake ,spinning nose devices and active blowing jet etc [9--13], have

* Associate Professor
\+ Engineer
** Associate Engineer

been presented.

In this paper, three experimental schemes of active control for asymmetric force in a low speed wind tunnel are discussed . The active control devices are designed. The control laws are investigated.

The experimental results show that the asymmetric forces at high incidence are reduced significantly for investigated schemes . The developed active control programs can automatically limit the side force on the model to its minimum magnitude. The schemes of controlable blowing jet and controlable strake can be adopted to enhanced the lateral maneuverability.

Model and Equipments

The experimental investigations for active control of asymmetric side forces at high incidence were carried out in a 1.5m open jet single circuit low speed wind tunnel at N.P.U.

In the investigated scheme of controlable rotating nose-tip,the model investigated, shown in Fig. 1a, is a 60mm diameter cylinder with tangent ogive nose.The slenderness ratio of the nose is 3.5. The total length of the model is 510mm. There is a rotating part at the tip of the model. The length of the rotating part is 60mm. The rotating nose tip is driven by a variable speed D.C. motor mounted in the model.

In the investigated scheme of controlable blowing jet, the model investigated, shown in Fig. 1b, is a 60mm diameter with a cone. The slenderness ratio of the nose is 3.5. The tatol length of the model is 530mm. There are several blowing holes at the nose. The diameter of the hole is 1mm.The blowing jet holes are connected to a high pressure air tank by plastic hose. The blowing jet rate is controled by a flow-regulation valve, which is driven by a servo-motor.

In the investigated schemes of controlable strakes, an aircraft model, shown in Fig.1c, is investigated. The fuselage of the model is a 80mm diameter cylinder with a tangent ogive nose (slenderness ratio= 3.5). The wing of the model is a planar wing with sharp edge. The aspect ratio of the wing is 2.2 and the sweepback angle at leading edge is 50° . The sweepback of the strake is 75° .The strake can rotate around the axis which is perpendicular to the fuselage axis. The deflection of the left and right strake are driven by two servo-motor mounted in the fuselage respectively.

The experimental speed of the wind tunnel is about 30 m/s. The Reynolds number base on freestream velocity and diameter of the model or the average aerodynamic chord of the wing is about $1.5*10^5$ or $6*10^5$. The model were sting-supported at their base.

The aerodynamic forces were measured by six-component mechanical-strain gauge balance. The vorticity distribution in the wake was measured by a photo-electric digital vorticity meter consisting of two major parts: a vane, shown in Fig. 2, and a digital frequency meter.

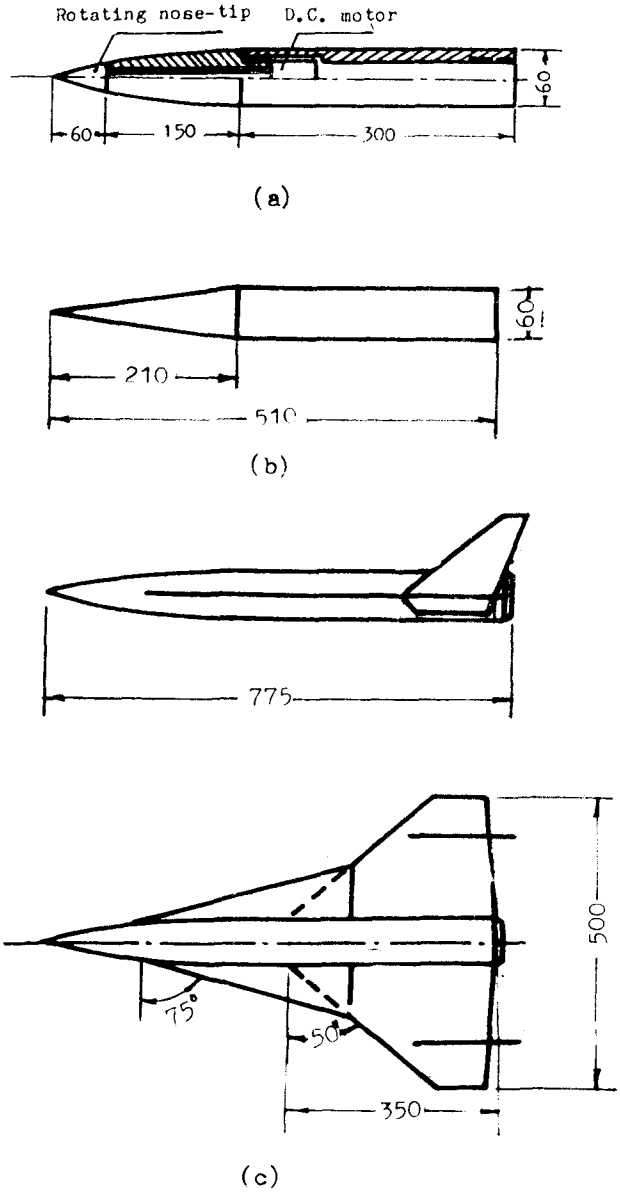

Fig. 1. Sketch of the models

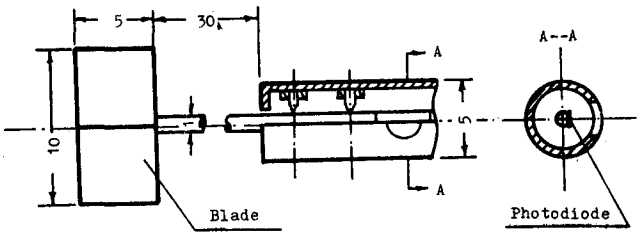

Fig. 2. Sketch of the vane for vorticity measurement

Active Control Device

The microcomputer is a main component of the active control device. The side forces(side force , yawing moment or rolling moment) elements of the balance were used as a side force sensor. The angle of attack sensor was connected to the angle-of-attack mechanism of the wind tunnel. The signals from these sensors were transformed to digital quantities by analog-to-digital converters and conveyed to the microcomputer. The digital output of the microcomputer was then reconverted to an analog signal to control the servo-motor. The control parameters (such as the rotating rate of the nose tip etc.) are adjusted properly and the asymmetric forces on the model can be reduced to minimum value (or increase to maximum value).

Two active control programs are adopted:

1. Function feedback control (F.F.C)
2. Adaptive control (A.C)

Their principles are briefly discussed as follows.

1. Function feedback control

The control parameter corresponding to minimum side force are measured beforehand at various angle of attack and the results are store in the microcomputer. When the signal of the angle of attack sensor is fed into microcomputer, it will send a previous specified signal to the servo-motor. Thus, the control parameter can be maintained the appropriate value,producing the minimum side force at each angle of attack. The block diagram of function feedback control is shown in Fig. 3a.

2. Adaptive control

When the control parameter varies continuously in their working range, both the side force on the model and the state of the servo-motor are recorded by the microcomputer. Thus, the state of the servo-motor corresponding to the minimum side force is found by microcoputer automatically. Thus, the state of the servo-motor is kept invarient and the minimum side force is obtained on the model. When angle of attack is changed , the process is repeated. Hence the minimum force on the model at each angle of the attack be obtained automatically.

The block diagrams of the active control device is shown in Fig. 3b.

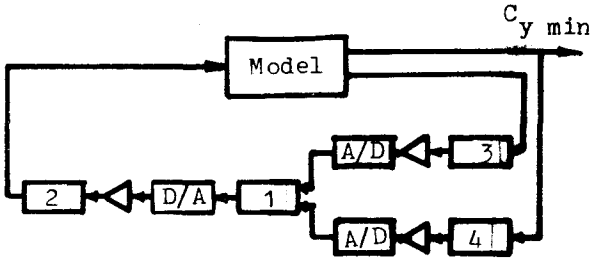

(a)

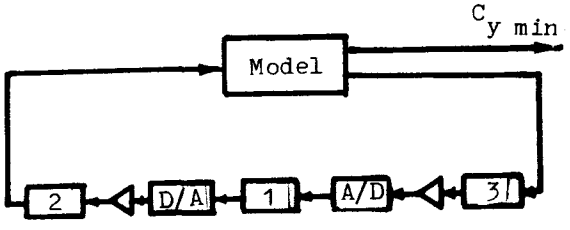

(b)

1.Microcomputer 2 Servo-motor
3.Angle of attack sensor
4.Side force sensor

Fig. 3. Block diagram
(a) function feedback control
(b) adaptive control

Results and Conclusions

To obtain the control law for active control of asymmetric forces at high incidence by wind tunnel test , the side forces were measured at each incidence various nose tip rotating speed, blowing jet rate and deflection of strake respectively. The results are shown in Fig. 4,5 and 6. From these data the relation between the control parameter corresponding to minimum side force and angle of attack, ie. the control law, can be found as shown in Fig. 7-9. The results show that the side forces can be reduced significantly for all investigated active control schemes,shown in Fig.10--16. The vorti-

city field on the lee side of the model are measured for schemes of the rotating nose-tip and blowing jet. The results are shown in Fig.17,and 18. It can be seen that the asymmetry of the wake vortex distribution are decreased significantly.

In same principle, when the control parameters corresponding to maximum side forces at various angle of attack and the results are stored in the microcomputer, the maximum side force on the model can be obtained and the lateral maneuverability can be enhanced. The experimental results are shown in Fig.19 and 20.The results are very interesting , because the efficiency of the traditional control surface, such as aileron, is very low at high angle of attack.

The influence of the rotating nose tip and blowing jet to longitudinal characteristics is insensitive and the influence of the controlable strake is significant shown in Fig.21,22,23 and 24

Base on above data, some conclusions can be obtained.

1. The asymmetric side forces can be reduced significantly for all investigated active control schemes.
2. The active control programs developed can be automatically limit the asymmetric side force on the model to their minimum magnitude.
3. The lateral maneuverability can be enhanced by controlable blowing jet and controlable strake schemes.
4. The influence of the rotating nose tip and blowing jet to longitudinal characteristics is insensitive and the influence of the strake is significant.

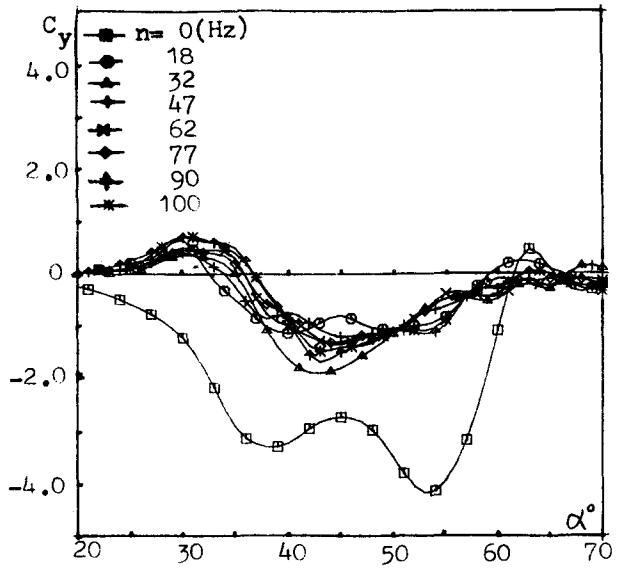

Fig. 4. Side force coefficient for different rotating rates

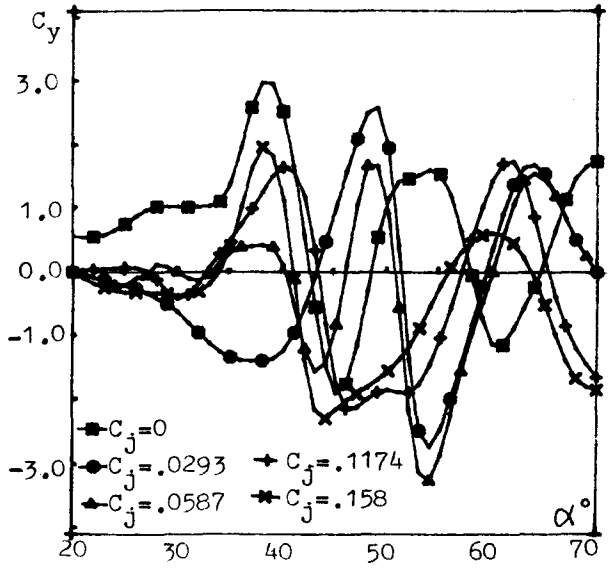

Fig. 5. Side force coefficient for different blowing jet rates

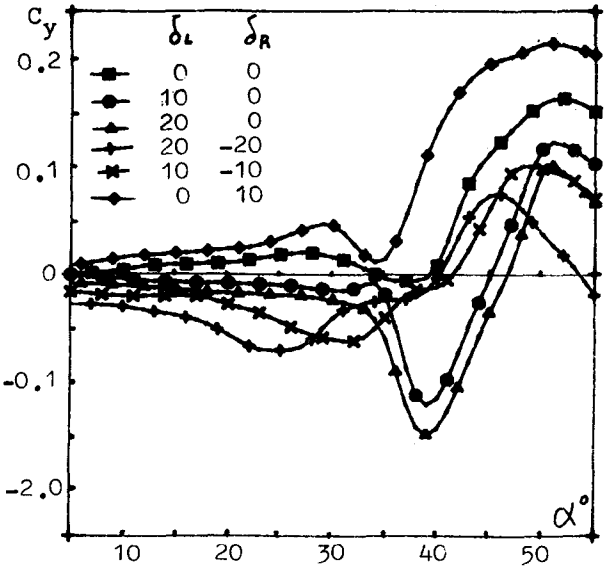

Fig. 6. Side force coefficient for different deflection of strake

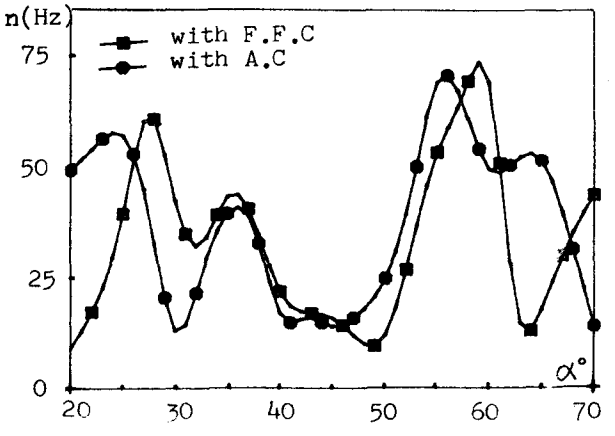

Fig. 7. Rotating rate corresponding to minimum side force

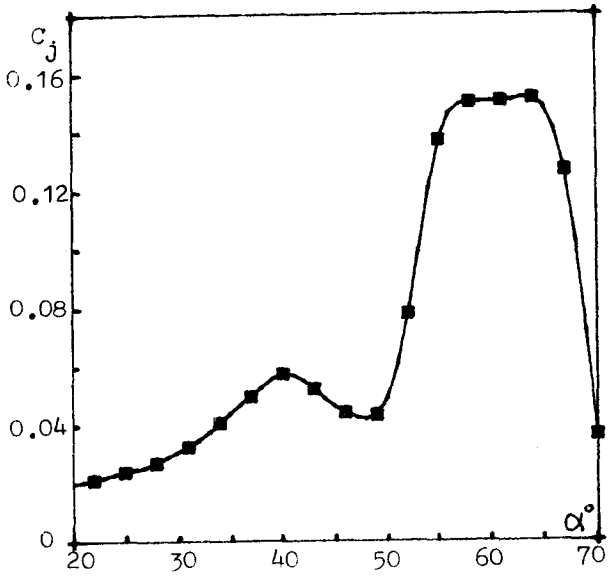

Fig. 8. Blowing jet rate corresponding to minimum side force

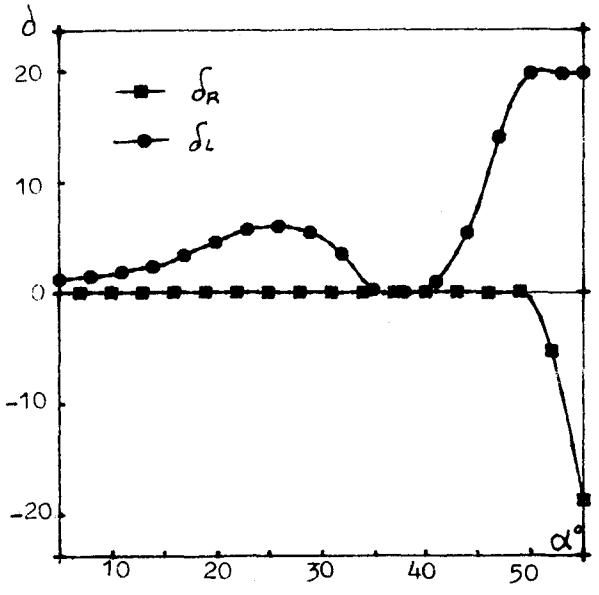

Fig. 9. Deflection of the strake corresponding to minimum side force

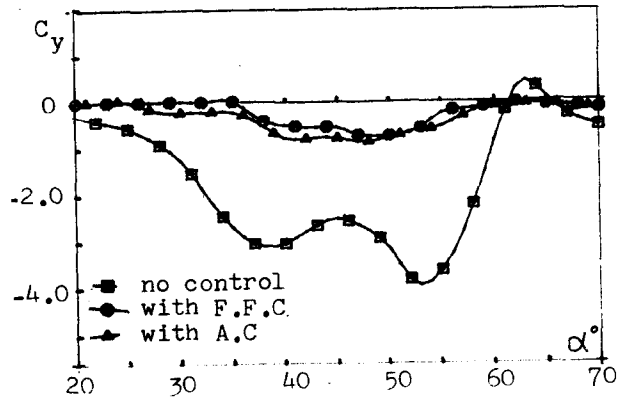

Fig.10. Side force coefficient with and without control (in scheme of the rotating nose)

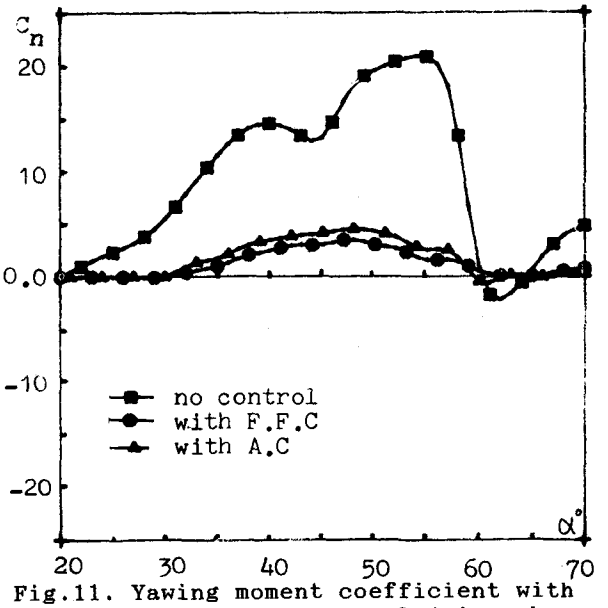

Fig.11. Yawing moment coefficient with and without control (in scheme of the rotating nose)

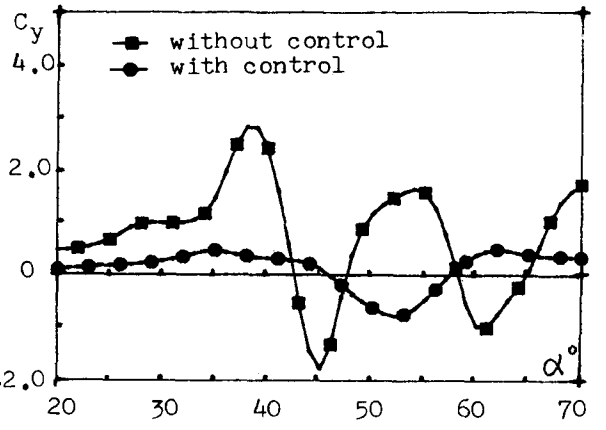

Fig.12. Side force coefficient with and without control (in scheme of blowing jet)

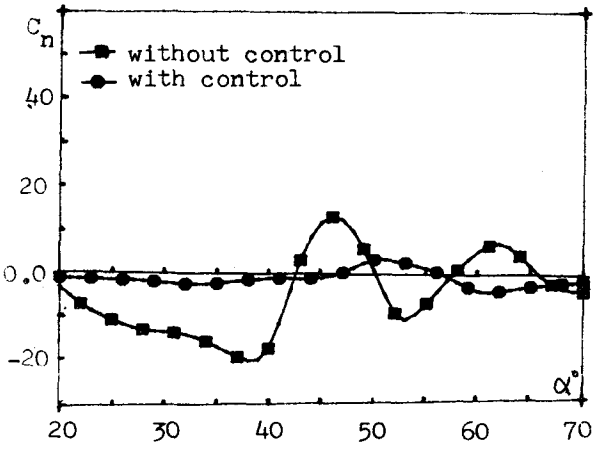

Fig.13. Yawing moment coefficient with and without control (in scheme of blowing jet)

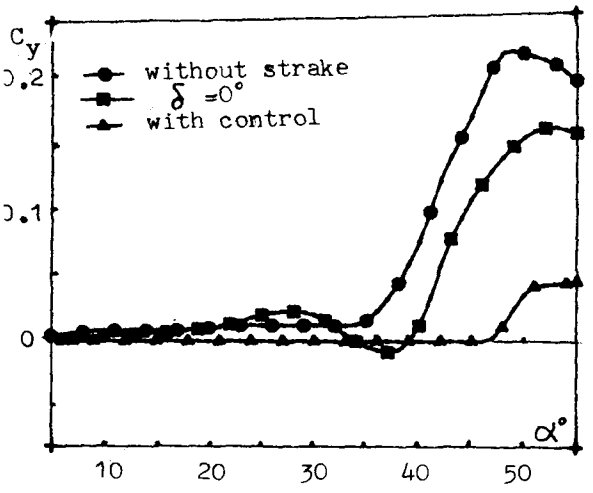

Fig.14. Side force coefficient with and without control (in scheme of controlable strake

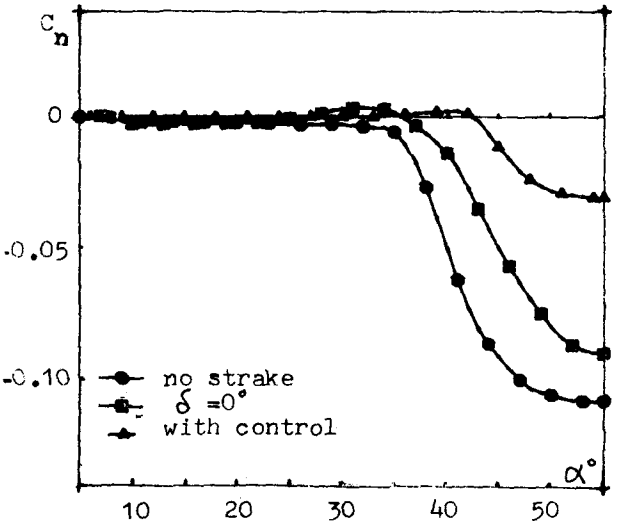

Fig.15. Yawing moment coefficient with without control (in scheme of controlable strake

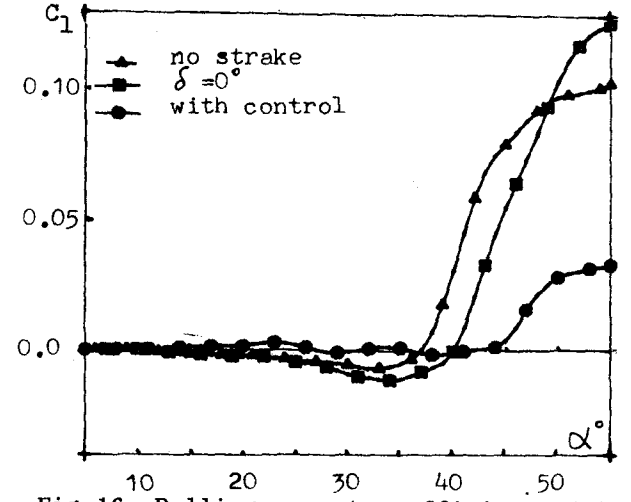

Fig.16. Rolling moment coefficient with without control (in scheme of controlable strake)

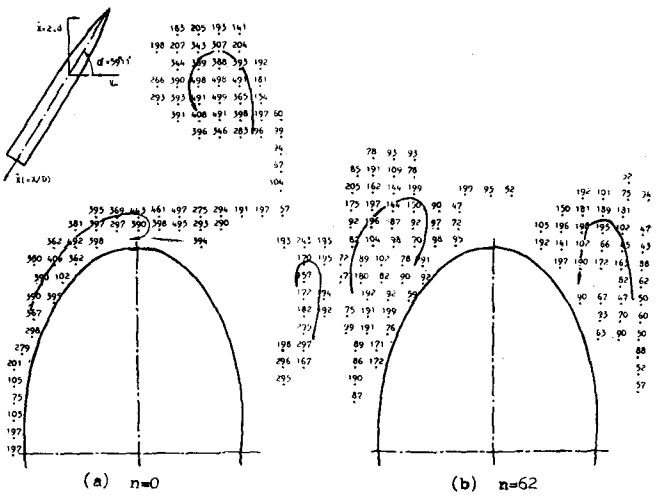

Fig.17. Wake vortices distribution x=2.8, α=59.2° (a) n=0 (b) n=62

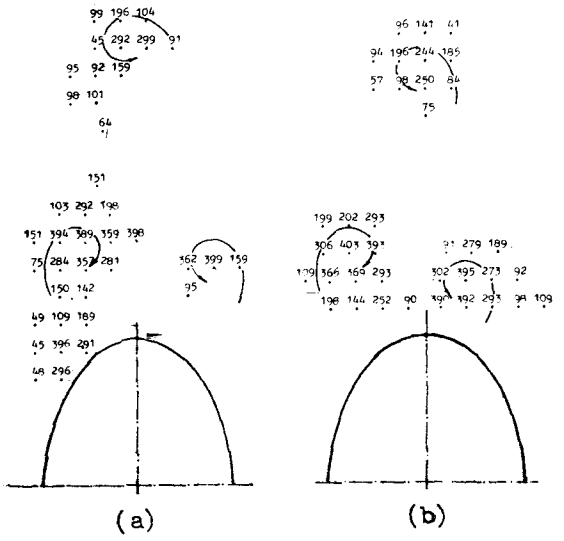

Fig.18. Wake vortices distribution x=1.5, α=35.1° (a) C_j=0 (b) C_j=.0424

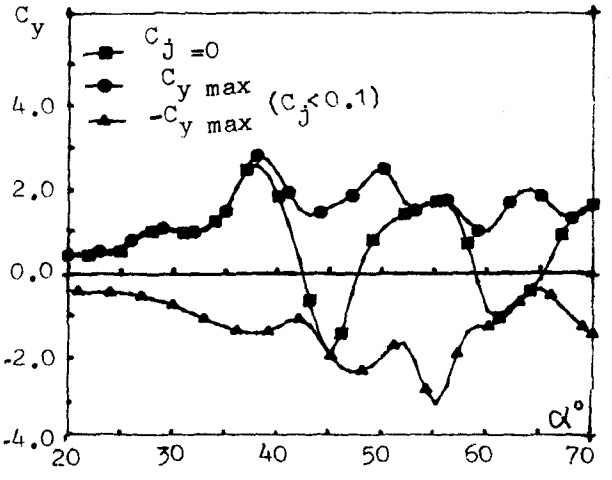

Fig.19. Blowing jet rate corresponding to maximum side ($C_j \leq 0.1$)

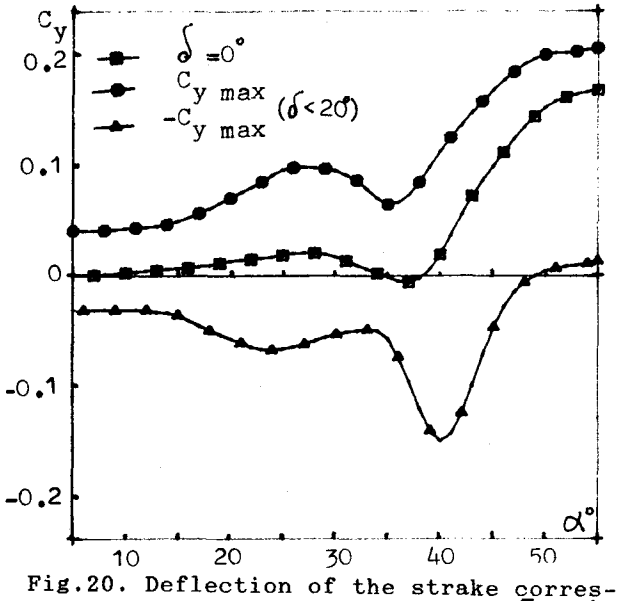

Fig.20. Deflection of the strake corresponding to maximum side ($\delta \leq 20°$)

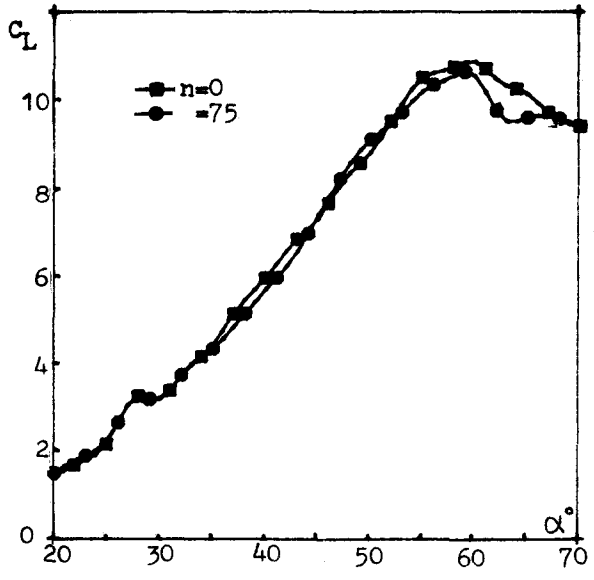

Fig.21. The influence of the rotating nose to lift coefficient

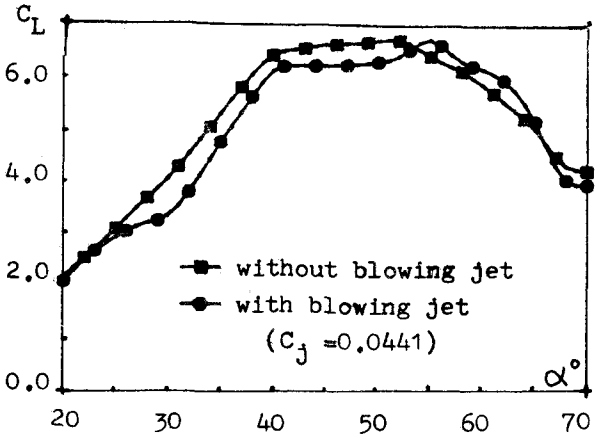

Fig.22. The influence of the blowing jet to lift coefficient

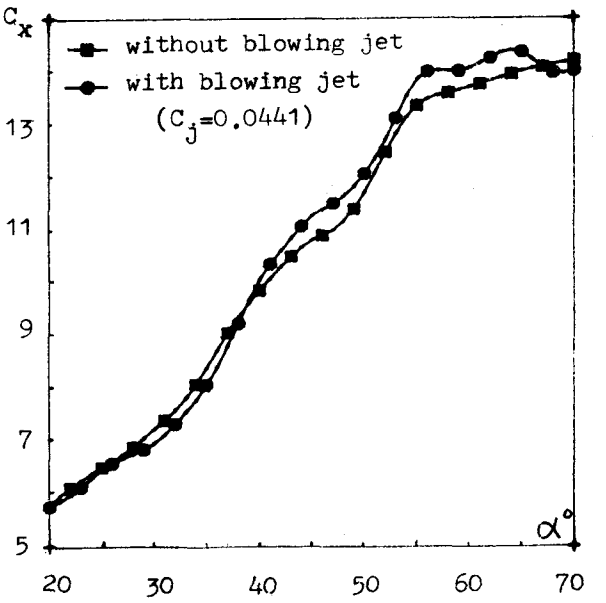

Fig.23. The influence of the blowing jet to resistance coefficient

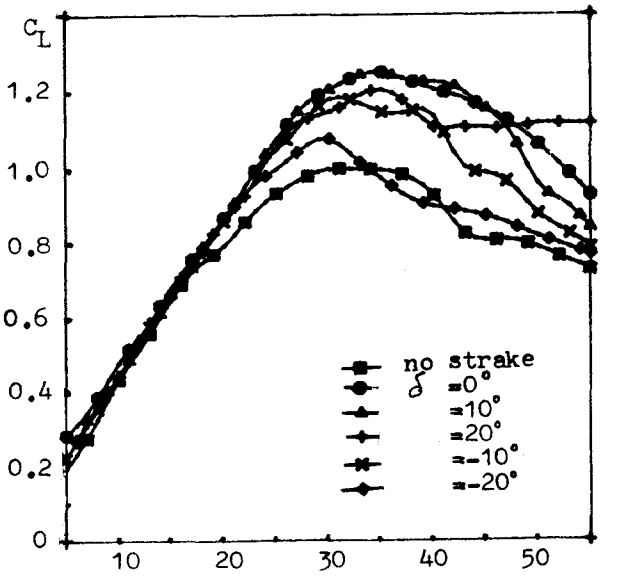

Fig.24. The influence of the deflection of strake to lift coefficient

Reference

1. Pick. G.S., "Side Forces on Ogive Cylinder Bodies at High Angles of Attack in Transonic Flow", Journal of Spacecraft and Rockets, Vol.9,June 1972, pp.389-390.
2. Moss, G.F.,"Some UK Research Studies of the Use of Wing-Body Strake on Combat Aircraft Configurations at High Angle of Attack",AGARD CP-247, 1979, PP.4.1-4.9.

3. Peake, D. J. and Owen, F. K., " Control of Forebody Three-Dimensional Flow Separations",NASA TM 78593, 1979.
4. Ericsson,L.E.and Reding,J.P., "Aerodynamic Effects of Asymmetric Vortex Shedding from Slender Bodies", AIAA Paper 85-1797,1985.
5. Modi, V.J.,Ries,T.,Kwan, A., and Leung, E.,"Aerodynamics of Pointed Forebodies at High Angle of Attack", Journal of Aircraft,Vol.21,June 1984, pp.428-432.
6. Almosnino D. and Rom, J.,"Lateral Forces on Slender Body and Their Alleviation at High Incidence " , Journal of Spacecraft and Rockets, Vol. 18,Sept-Oct. 1981, pp.393-400.
7. Jorgensen, L . H . and Nelson,E.R., "Experimental Aerodynamic Charateristics for a Cylindrical Body of Revolution with Various Noses at High Angle of Attack from 0 to 58 deg and Mach Number from 0.6 to 2.0 ", NASA TM X-3128,1974.
8. Luckring, J.M., "Theoretical and Experimental Aerodynamics of Strake Wing Interactions up to High Angle-of-Attack", AIAA Paper 78-120,1978.
9. Rao,D.M. and Huffman, J.K., "Hinged Strakes for Enhanced Maneuverability at High Angle of Attack" , Journal of Aircraft, Vol.19, April 1982, pp. 278-282.
10. Kruse, R.L., "Influence of Spin Rate on Side Force of an Axisymmetric Body",Journal of Aircraft,Vol. 16,April 1978, pp.415-416.
11. Fidler, J.E., "Active Control of Asymmetric Vortex Effects",AIAA Paper 80-0182, 1980.
12. Yang, Y-N," The Alleviation and Control of the Asymmetric Load at High Angle of Attack ",Acta Aerodynamica Sinica, No. 1,March 1985, pp.112-116.
13. Yang Y-N et al. "Active Control of Asymmetric Force at High Incidence", Journal of Aircraft, Vol.25 ,No. 2. 1988.